Stochastic trade-offs and the emergence of diversification in *E. coli* evolution experiments

Roberto Corral López,[1] Samir Suweis,[2,3] Sandro Azaele,[2,3,4,*] and Miguel A. Muñoz[1,*]

[1]*Departamento de Electromagnetismo y Física de la Materia and Instituto Carlos I de Física Teórica y Computacional, Universidad de Granada, E-18071 Granada, Spain*

[2]*Dipartimento di Fisica e Astronomia Galileo Galilei, Università degli Studi di Padova, via Marzolo 8, 35131 Padova, Italy*

[3]*Istituto Nazionale di Fisica Nucleare, 35131 Padova, Italy*

[4]*National Biodiversity Future Center, Piazza Marina 61, 90133 Palermo, Italy*

(Received 23 July 2024; accepted 4 October 2024; published 25 November 2024)

Laboratory experiments with bacterial colonies under well-controlled conditions often lead to evolutionary diversification, where at least two ecotypes emerge from an initially monomorphic population. Empirical evidence suggests that such an "evolutionary branching" occurs stochastically, even under fixed and stable conditions. This stochasticity is characterized by (i) the occurrence of branching in a significant fraction, but not all, of the experimental settings, (ii) the emergence at widely varying times, and (iii) variable relative abundances of the resulting subpopulations across experiments. Theoretical approaches to understanding evolutionary branching under these conditions have been previously developed within the (deterministic) framework of "adaptive dynamics." Here, we advance the understanding of the stochastic nature of evolutionary outcomes by introducing the concept of "stochastic trade-offs" as opposed to "hard" ones. The key idea is that the stochasticity of mutations occurs in a high-dimensional trait space and this translates into variability that is constrained to a flexible tradeoff curve in a lower-dimensional space. By incorporating this additional source of stochasticity, we are able to account for the observed empirical variability and make predictions regarding the likelihood of evolutionary branching under different experimental conditions. This approach effectively bridges the gap between theoretical predictions and empirical observations, providing insights into when and how evolutionary branching is more likely to occur in laboratory experiments.

DOI: 10.1103/PhysRevResearch.6.043199

I. INTRODUCTION

Understanding the origin and evolution of biological diversity is one of the central issues in evolutionary biology [1–3]. Historically, diversification was primarily understood in the context of *allopatry*, resulting from geographical isolation between subpopulations of a common ancestral species [4–8]. However, in recent years there has been a shift to the consideration of *sympatric* diversification, which occurs without spatial segregation. This has been driven by mounting empirical evidence from both field and laboratory experiments [9–22] as well as by the consolidation of adaptive dynamics theory as a robust theoretical framework for addressing this type of eco-evolutionary problem [23–31].

In the theory of adaptive dynamics, diversification is understood as the consequence of *evolutionary branching*, where two phenotypically distinct populations emerge from an ancestral monomorphic one (see [23–27] and below). Adaptive dynamics assumes the presence of a "resident population," usually considered to be monomorphic, from which "mutants" of the dominant phenotype emerge at a small rate. This small mutation rate ensures that ecological and evolutionary processes occur on separate timescales. These concepts are mathematically encapsulated in the notion of *invasion fitness*, which describes the dependence of a mutant's growth rate on the resident population. Specifically, the sign of this growth rate determines whether the mutant will go extinct or proliferate, eventually invading the resident population and becoming fixed. Thus, adaptive dynamics can be seen as the gradual phenotypic change of an entire population, evolving uphill in the fitness landscape [23,24]. Importantly, owing to the frequency-dependent nature of the invasion fitness, the fitness landscape is a dynamic entity that changes as the population composition changes in phenotypic space.

Typically, this evolutionary process culminates in finding a (local) maximum of the fitness landscape, where the population stabilizes. However, sometimes it may result in the counterintuitive phenomenon of evolutionary branching. This occurs when the endpoint of the gradient-ascending dynamics, which simultaneously modifies the fitness landscape itself, is a fitness *minimum* rather than a maximum [23–27]. At this type of "singular point," the population can only increase its overall fitness by splitting into two subpopulations. Each subpopulation can then separately ascend one side of the fitness landscape, resulting in diversification into two distinct lineages [23,24,27,32–34].

This form of adaptive diversification has been empirically observed in a myriad of experiments. For instance, isogenic

*These authors contributed equally to this work.

and well-mixed populations of *E. coli* have been reported to evolve into (at least) two coexisting ecotypes with different carbohydrate metabolisms, both in chemostats [14–16] and in serial-dilution (batch) experiments [10,11,17,35–38]. In chemostats, where the bacterial population is continuously fed solely with glucose, one emerging subpopulation specializes in consuming glucose, while the second specializes in scavenging acetate, a typical byproduct of glucose metabolism. Conversely, in serial dilution experiments where both glucose and acetate are added in cycles of serial dilutions, the difference between the emerging phenotypes lies in the time lag required to switch to acetate consumption when glucose becomes depleted. For example, Treves *et al.* [16] reported that 6 out of 12 independent replicate evolutionary experiments in a chemostat resulted in a stable polymorphism for up to 1750 generations. Similarly, Friesen *et al.* [10] observed clear dimorphism in 5 out of 12 independent replicate serial-dilution experiments after 1000 generations.

It is worth noting that despite the inherent stochasticity of mutations, evolutionary branching turns out to be quite reproducible, with a significant proportion of trials resulting in stable dimorphism [10,13,14,16,36]. Nevertheless, significant trial-to-trial variability is also observed; in particular, (i) diversification is reported in a large fraction, but not all, of the experiments, (ii) it happens at broadly diverse times, and (iii) the population fraction of the two emerging ecotypes is variable across experiments [16].

Prior theoretical analyses within the adaptive dynamics framework have demonstrated that simplified eco-evolutionary models can undergo evolutionary branching under the described conditions [10,31]. However, these approaches are deterministic in nature, leading to the prediction of branching occurring in all or none of the realizations based on certain modeling assumptions or parameter values. Specifically, to replicate branching, previous studies relied on the arbitrary selection of a mathematical function to represent a "trade-off" between the different metabolic choices to be optimized, while alternative choices of the trade-off curve did not result in branching [10,31].

Trade-offs, often encapsulated by the idea that "you cannot be good at everything," are fundamental in ecological and evolutionary modeling [39]. Typically, hard trade-offs, prevalent in modeling, reflect the notion that evolutionary pressures drive organisms toward a Pareto front [40]. Here, improvements in one task come with a cost to efficiency in others [41]. In our context, a specific trade-off curve has been commonly assumed between the abilities to metabolize glucose and acetate. However, selecting a precise trade-off curve is often the least justified aspect of mathematical models. While conceptually well founded, the experimental measurement of trade-offs presents significant challenges [42,43]. Furthermore, as extensively debated in the literature, the choice of a specific trade-off curve is pivotal as it fundamentally dictates the occurrence or absence of evolutionary branching [24,44]. An elegant solution to circumvent this conceptual challenge within the adaptive dynamics framework was proposed by de Mazancourt and Dieckmann [44]. They devised a strategy to assess, for any given eco-evolutionary model, the robustness of the potential for evolutionary branching as the mathematical form of the trade-off function is altered (see below).

Our main goal here is to provide a theoretical and computational framework to account for the observed variability in the outcomes of controlled evolutionary-branching experiments. We aim to achieve this by introducing the concept of "stochastic" trade-offs, contrasting with the conventional "hard" trade-offs, within the adaptive dynamics framework. Here, stochastic trade-off implies that the population is not bound to evolve along a rigid, predefined curve (Pareto front) in phenotypic space, as is the case with hard trade-offs. Instead, it operates within a more flexible and extended region, allowing for greater exploration of phenotypic diversity. As we will show, by adjusting the width of this region, which reflects the flexibility of the underlying bacterial metabolic constraints, it is possible to effectively regulate the degree of variability.

Let us remark that very recent theoretical works have also reported variability in the emergence of diversification across replicates [45,46]. In particular, in [45], the strict trade-off is replaced by an upper bound for the consumption rates of the different resources (i.e., the metabolic traits) and the authors investigate the effect of clonal interference (i.e., strong mutations [47]) and its role in fostering diversification under varying mutation rates. Conversely, in [46], the authors examine the interplay between selection and diversification by controlling the relative rates of purely fitness mutations and resource-strategy mutations, exploring the resulting regimes. Thus, in both studies, variability in diversification is controlled by mutation rates. We also find that larger mutation rates (beyond the infinitesimally small mutation limit) enhance variability. However, in contrast to previous studies, we propose an alternative source of variability that is independent of changes in the mutation rate: a stochastic trade-off model, where variability arises from the presence of a high-dimensional trade-off manifold representing the underlying metabolic constraints between all evolution-susceptible variables. Specifically, in our approach, the variability of metabolic traits in the high-dimensional manifold is captured by a stochastic evolution of phenotypic traits in a lower-dimensional space (see below).

Given the limited availability of experimental data, it is challenging to determine which mechanism best accounts for the observed variability, and it is also possible that multiple factors may contribute. However, we believe that the framework we introduce is especially well suited for investigating this problem because (i) we utilize a biologically realistic ecological model fed with empirically fitted data to quantitatively describe the chemostat experiments [14–16] (although the concepts could also be extended to analyze serial-dilution experiments), (ii) we propose a straightforward extension of the well-known framework of adaptive dynamics by adding stochasticity into the trade-off, which allows for a controlled inclusion of variability, (iii) we generalize our results for a large family of trade-off curves, and (iv) we formulate additional theoretical predictions about the emergence of diversification under varied experimental scenarios.

The paper is structured as follows: Section II introduces the eco-evolutionary model and defines the concept of stochastic trade-offs. Section III outlines the main findings, while Sec. IV offers conclusions and delineates future research avenues.

II. ECO-EVOLUTIONARY MODEL BUILDING

A. Ecological dynamics

To gain insight into the results of *E. coli* evolution experiments in chemostats, we first construct a simple yet biologically realistic ecological model, inspired by existing modeling approaches [31,48,49]. This model aims to quantitatively describe the bacterial population and integrate key aspects of the experimental setups [14–16]. Specifically, it encompasses the following components and characteristics:

(i) Initially, the bacterial population is monomorphic, consisting of a large number of phenotypically identical individuals (of the order of 10^{13} cell L^{-1} [48]), and it is cultured in a glucose-limited chemostat [15,16].

(ii) Under the conditions of the experiment, when bacteria metabolize glucose, they produce acetate due to overflow metabolism (a phenomenon where fermentation is preferred over respiration). This results in the excretion of acetate in proportion to the amount of glucose that is consumed [15,50].

(iii) The excreted acetate acidifies the medium, which leads to an overall slowing down of the total population growth rate [48].

(iv) Even if a strain emerges with the ability to metabolize acetate, its consumption is typically repressed in the presence of glucose, which is the preferred resource [49].

Considering these ingredients, one can write the following set of (deterministic) differential equations for the total number of cells, $N(t)$, and the concentrations of glucose, $G(t)$, and acetate, $A(t)$, respectively, that represent the ecological (not evolutionary) part of the dynamics:

$$\frac{dN}{dt} = \gamma\left(V_g\frac{G}{K_g+G} + V_a\frac{A}{K_a+A}\frac{C_g}{C_g+G}\right)\frac{C_a}{C_a+A}N - DN, \tag{1}$$

$$\frac{dG}{dt} = D(G_0 - G) - V_g\frac{G}{K_g+G}N, \tag{2}$$

$$\frac{dA}{dt} = \beta V_g\frac{G}{K_g+G}N - V_a\frac{A}{K_a+A}\frac{C_g}{C_g+G}N - DA. \tag{3}$$

Observe first that all growth kinetics are described using Monod's functions [51]. For example, $V_g\frac{G}{K_g+G}$ ($V_a\frac{A}{K_a+A}$) represents the consumption of glucose (acetate) at a maximum growth rate per capita V_g (V_a) and half-saturation constant K_g (K_a). The factor involving C_g controls the repression of acetate consumption due to the presence of glucose, while the one with C_a represents the inhibition of overall growth caused by acetate-induced acidification of the medium. γ is the conversion constant for biomass production from resources, β determines the fraction of consumed glucose excreted as acetate, D is the chemostat's dilution rate, and G_0 is the rate at which glucose is supplied to the chemostat. The corresponding numerical values of all these parameters are taken from experimental measurements [14–16] and are specified in the Supplemental Material (SM), Table I [53].

Thus, in a nutshell, the population N increases due to the consumption of glucose and/or acetate. However, consumption of acetate is inhibited due to catabolite repression and overall growth is limited due to the acidification of the medium caused by acetate.

B. Evolutionary dynamics

To complete the eco-evolutionary model, we must define the evolutionary part of the dynamics. This involves determining which ecological parameters [e.g., constants in Eqs. (1)–(3)] are subject to change over time and which remain constant throughout the evolutionary process. Based on experimental findings [14–16], it is evident that the abilities to metabolize both glucose and acetate evolve over the course of the experiments. Therefore, parameters such as $V_{a,g}$, $K_{a,g}$, and C_g are all potential candidates for evolution. For the sake of simplicity, we opt for V_g and V_a—the maximum growth rates in glucose and acetate, respectively, represented collectively as $\mathbf{V} = (V_g, V_a)$—to serve as evolving parameters. These parameters are allowed to vary across generations, defining the *metabolic strategy* of each strain.

To incorporate evolution using adaptive dynamics, it is assumed that once the ecological dynamics reach a steady state [i.e., a state where Eqs. (1)–(3) with $\mathbf{V} = (V_g, V_a)$ stabilize], a "mutation" occurs. This implies that ecological and evolutionary processes are considered to occur at well-separated timescales. This mutation generates an individual mutant with a slightly different phenotype, $\mathbf{V}' = (V_g', V_a') \neq (V_g, V_a)$. The invasion fitness of this mutant, defined as its per capita growth rate within the existing resident population, can be expressed [from Eq. (1)] as

$$f(\mathbf{V}', \mathbf{V}) = \gamma\left(V_g'\frac{G^*}{K_g+G^*} + V_a'\frac{A^*}{K_a+A^*}\frac{C_g}{C_g+G^*}\right) \times \frac{C_a}{C_a+A^*} - D, \tag{4}$$

where G^* and A^* represent the steady-state values of the glucose and acetate concentrations, respectively, which depend on the values of both V_g and V_a of the resident population.

Using the formalism of adaptive dynamics, in the (deterministic) limit of small mutations, the evolution in phenotypic space is determined by the *canonical equation*, describing how the average phenotype in the population climbs up the fitness landscape [26,27,30],

$$\frac{d\mathbf{V}}{dt} = \mu\nabla_{\mathbf{V}'}f(\mathbf{V}', \mathbf{V})\Big|_{\mathbf{V}'=\mathbf{V}}, \tag{5}$$

where $\nabla_{\mathbf{V}'} = [\frac{\partial}{\partial V_1'}, \frac{\partial}{\partial V_2'}]$ is the fitness gradient and μ is the mutation rate, which in the simplest case adopted here is just a constant.

At this point, a specific trade-off function, denoted as $V_a = h(V_g)$, is typically introduced. This function reflects the biological fact that enhancing one metabolic strategy comes at the expense of efficiency in the consumption of the other, so that both strategies cannot be altered independently [39]. This implies that the canonical equation [Eq. (5)] needs to be modified by an additional term to account for such a hard constraint, as specified in the SM, Eq. (1) [53]. Analyzing the fixed points of the resulting equation, along with the properties (first and second derivatives) of the modified fitness gradient at these points, one could determine whether the course of

evolution (in the deterministic limit) leads to an evolutionarily stable population or to the emergence of evolutionary branching [52].

As discussed in Sec. I and explicitly demonstrated in Sec. III, the previously described adaptive-dynamics model coupled with a hard trade-off is deterministic. This means that it either exhibits branching for every model realization or it does not for any, depending on the specific shape of the considered trade-off curve. Consequently, it fails to elucidate the observed variability in the experiments such as the timing of diversification (branching) events and the proportion of the two emerging ecotypes over time. Let us remark that stochastic effects in the context of adaptive dynamics have already been considered in the literature. Wakano and Iwasa [54] (and, more recently, some of us [34]) have shown that finite-size effects in the population number may prevent the system from undergoing evolutionary branching, even though it is theoretically predicted to emerge at a deterministic level. However, these effects become negligible for the very large population sizes under consideration (here, $N \sim 10^{13}$).

To address stochasticity, we adopt a different approach. As stated in Sec. I, we are interested in explaining properties of the evolutionary experiments such as the time at which a diversification (branching) event occurs and the fraction of the two emerging ecotypes at a certain time. Therefore, we need to build a framework capable of reproducing actual stochastic evolutionary trajectories that follow, on average, the behavior described by the canonical equation, but also allow for variability.

Ideally, one would aim to construct a bottom-up approach by defining an individual-based model where each individual has its own associated phenotype, allowing for evolution through the combined processes of mutation and selection to occur [26,34]. However, given the size of empirical populations, typically around $N \sim 10^{13}$, such a "microscopic" description is currently computationally unfeasible. Therefore, as an alternative, we employ a framework adapted from [55] (see Sec. III of the SM [53]), which represents an effective "mesoscopic" description of the evolutionary trajectories. This approach does not directly deal with individual organisms but rather with "groups" of them (subpopulations) that share the same phenotype, i.e., individuals are clustered in groups and one writes dynamical equations for the abundances of such groups. Essentially, this involves considering a collection of possible coexisting subpopulations, which necessitates (i) expanding the set of ecological equations to account for multiple subpopulations instead of just one, (ii) running the ecological dynamics for a sufficiently large time as to reach a steady state, (iii) introducing an additional equation for a new mutant subpopulation whose phenotype slightly differs from the subpopulation from which it derives, and (iv) iterating this eco-evolutionary process.

Two remarks are in order before proceeding: First, let us recall that this framework, where the ecological dynamics reach stationarity before new mutations appear —as customarily assumed in adaptive dynamics [27]— corresponds to the strong-selection weak-mutation regime [47]. Note that for very large bacterial populations such as those studied here, the number of mutations per unit time in the entire population might be high [47]. Thus, the key implicit assumption is that even if generic mutations occur at a high rate, those directly affecting pathways involving the metabolism of acetate and glucose are much rarer, allowing us to assume a large separation of timescales between the ecological and evolutionary dynamics. Experimental findings support this assumption, showing that all acetate-scavenging strains acquired their ability to metabolize acetate through mutations in a specific gene [16]. Therefore, although the overall mutation rate might be high, mutations impacting that particular gene are much less frequent.

Second, to achieve the strict limit of perfect timescale separation in computational analyses, one would need to run the ecological dynamics for an arbitrarily long time to ensure that a steady state has been reached. Since the simulation time is necessarily finite, what one actually analyzes is a limit of a small, but not infinitely small, mutation rate, i.e., a weak (but not infinitely weak) mutation limit. This is why the algorithm accommodates a set of possible subpopulations, i.e., a distribution in phenotypic space, instead of a single population. In any case, one can perform analyses by progressively expanding the time of the ecological dynamics to verify that the resulting distributions become sharper as the time scale is enlarged.

C. Stochastic trade-offs

Here we introduce an additional source of stochasticity to account for the experimental variability. Specifically, we suggest the concept of a stochastic trade-off, wherein the population is not confined to a fixed trade-off curve in phenotypic space, but can instead wander within a broader region with fuzzy boundaries [56].

The concept of stochastic tradeoff can be rationalized as follows (see, also, Fig. 1). The underlying metabolic constraints of bacteria are indeed the same for every realization of the evolutionary experiments. However, such constraints involve complex relations between the many variables that are susceptible to evolution. In our case, we explicitly consider the evolution of V_g, V_a but, in principle, there are many other variables, denoted generically as $\vec{v}$, that could be affected by overall (energetic, metabolic, etc.) constraints. These intricate relationships can be mathematically modeled as a multidimensional constraint manifold, akin to a high-dimensional "Pareto front" as depicted in Fig. 1 [39,40]. In other words, the actual trade-off involves a high-dimensional manifold, rather than the two-dimensional one characterizing metabolic preferences.

In such a framework, different experimental realizations, originating from the same point in the high-dimensional manifold (or Pareto front), can produce diverse trajectories that diverge along distinct paths inside the manifold due to the emergence of different mutations, which are intrinsically stochastic. Therefore, as illustrated in Fig. 1, the evolutionary trajectories when projected in the two-dimensional (V_g, V_a) plane are generally not confined to a one-dimensional curve and they may vary across experimental realizations. It is thus reasonable to consider the effect of metabolic constraints as defining a wide region in the lower-dimensional space of metabolic preferences, rather than as a strict (one-dimensional) curve.

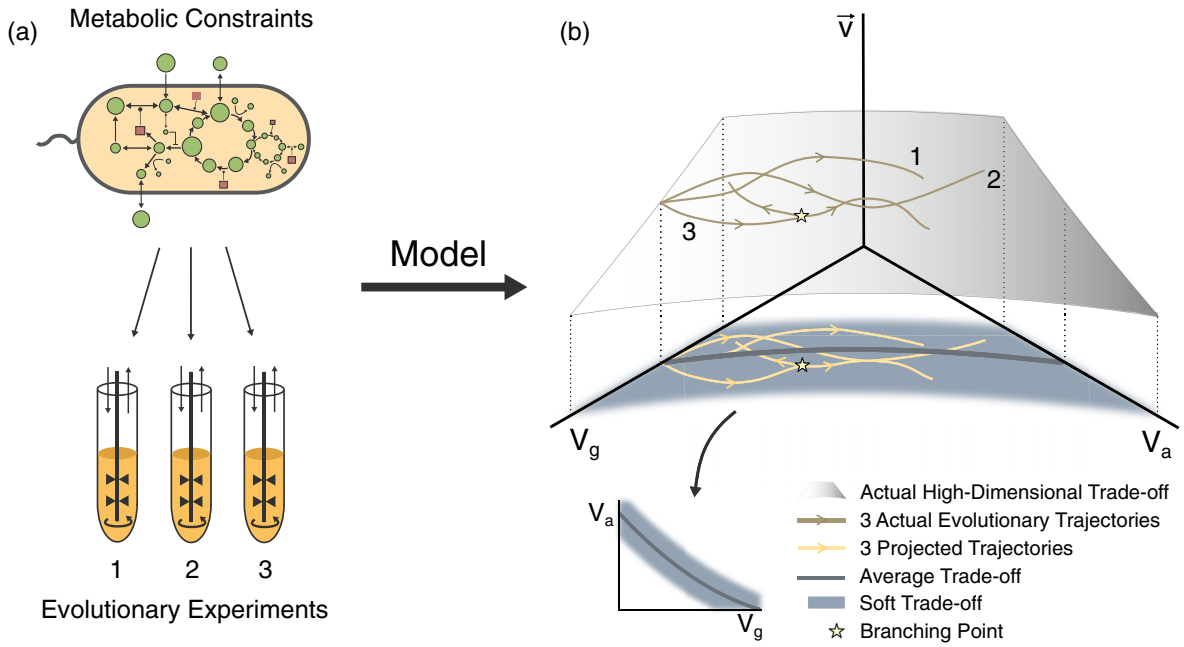

FIG. 1. Schematic representation of the concept of stochastic trade-off. (a) Metabolic constraints of bacteria influence the outcome of evolutionary experiments. (b) These constraints can be represented by a (topologically complex) manifold (gray shadowed surface), in the multidimensional space formed by all the relevant variables for evolution, which in our case are V_g, V_a and the rest, v. Starting from the same point, the different evolutionary trajectories corresponding to different realizations of the experiments can move freely in the high-dimensional constraint manifold (golden curves), possibly giving rise to diversification events if they reach a singular point (yellow star). Thus, the trajectories projected in the (V_g, V_a) plane (yellow lines) are restricted to a certain zone (blue area), but can be different from each other. We model this constraint region, that is, the stochastic trade-off in the lower-dimensional manifold, by adding a temporarily correlated noise on top of a certain fixed curve that stands as the average of possible trajectories (inset plot).

More specifically, we describe these constraints in the (V_g, V_a) plane as a stochastic process (modeled as an Ornstein-Uhlenbeck process with amplitude σ and temporal correlation τ, as explicitly shown in Sec. II of the SM [53]), added as an orthogonal perturbation to some central trade-off curve. This curve stands as the average of trajectories and can be chosen with large flexibility without affecting the conclusions (see Sec. II of the SM [53]). Depending on the amplitude and temporal correlations of the additional stochasticity, trajectories are constrained to wander at tunable distances of the central trade-off curve, allowing us to model the flexibility of the metabolic constraints in the (V_g, V_a) plane and, in turn, the variability of the trajectories.

It is important to note that although selection in the two-dimensional phenotypic plane tries to push trajectories away from the average curve in the direction of increasing fitness, where both V_g and V_a grow, our model "forces" the trajectories to stay close to the average curve. This serves as an effective way to model the constraints arising from the higher-dimensional manifold where mutations can have a positive, negative, or neutral effect when projected onto the $(V_g - V_a)$ plane.

In summary, the stochastic trade-off allows for the population to navigate and randomly explore a broad phenotypic region [in the (V_g, V_a) plane], effectively capturing the impact of metabolic constraints, rather than being restricted to a fixed trade-off curve.

III. RESULTS

A. Reproducibility and variability of experimental results

As illustrated in Fig. 2, computational analyses of the eco-evolutionary (mesoscopic) model coupled with a stochastic trade-off (as defined in Sec. II of the SM [53]) reveal that it is able to account for evolutionary branching as well as for the variability evinced in the experiments [16]. In particular, Figs. 2(a)–2(c) shows three temporal snapshots of the evolution of the population in phenotypic space for a specific realization of the model with the stochastic trade-off [as illustrated in the inset of Fig. 2(b)] that ended up diversifying in two highly specialized subpopulations.

Figure 2(a) represents the initial phase of the evolutionary picture, in which a glucose-specialist population that produces acetate evolves its ability to assimilate acetate because it is evolutionarily favored, so that it starts moving progressively "uphill." Figure 2(b) shows the phase in which the population has accumulated some variability and—upon arriving to a singular point—splits in two main ecotypes due to disruptive selection: one more specialized in acetate and the other still relying predominantly on glucose consumption. Figure 2(c) illustrates the final phase, where the two branched types diverge, each becoming increasingly specialized in metabolizing one of the two carbon sources. This divergence thus gives rise to the two distinct ecotypes observed in the experiments: the glucose specialist and the acetate scavenger. This

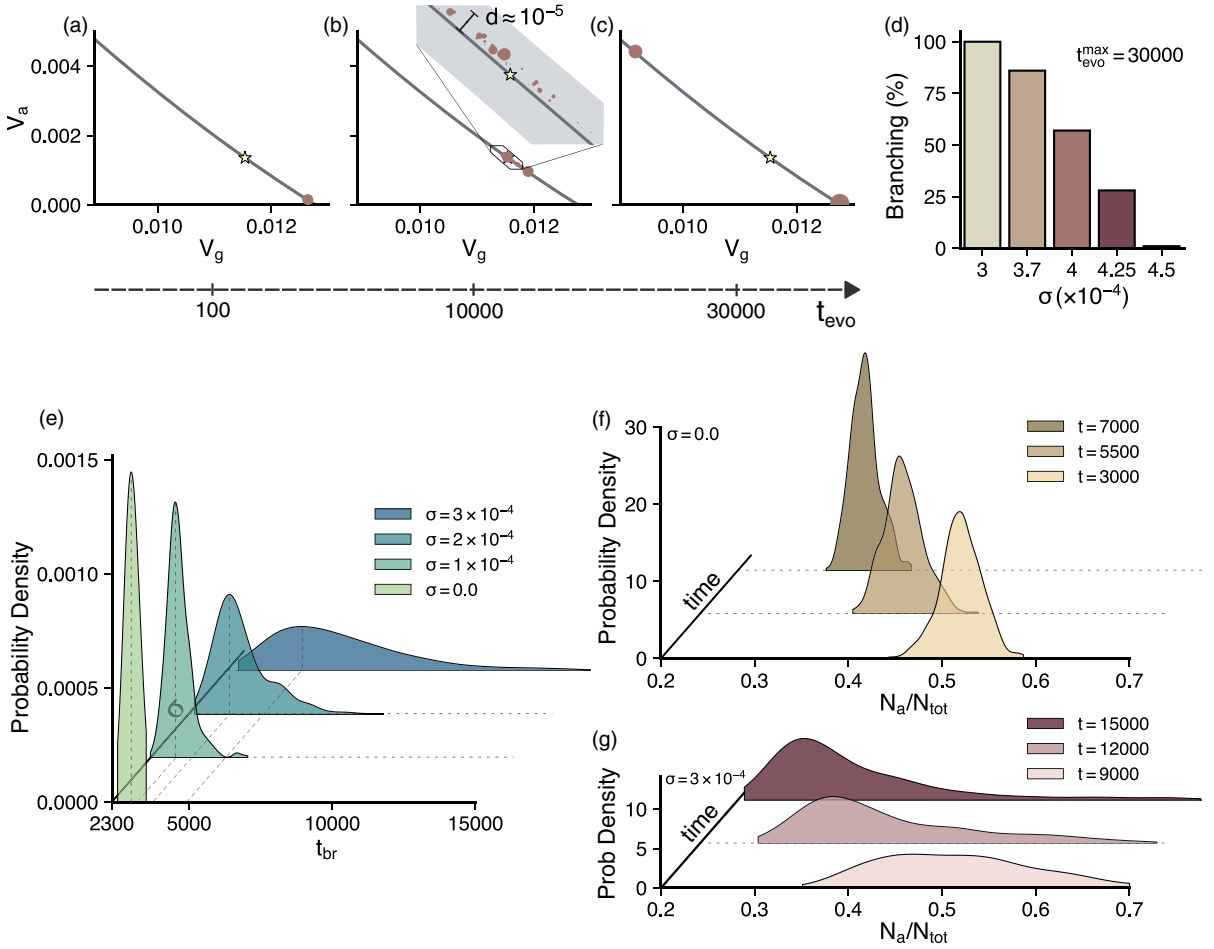

FIG. 2. Reproducibility and variability of evolutionary branching in our mesoscopic model with a stochastic trade-off. (a)–(c) Subpopulations in phenotypic space (represented by a red circle whose radius is proportional to its abundance) for three different times along the evolutionary trajectory, i.e., (a) before branching, (b) during branching, and (c) after branching, for one specific realization with $\sigma = 4 \times 10^{-4}$. The inset in (b) is a zoom in the region close to the branching point (yellow star), where $d \approx 10^{-5}$ is the maximum distance from a subpopulation to the average of the stochastic trade-off. (d) Percentage of realizations (number of them $N_r = 200$) that undergoes evolutionary branching for different amplitudes of the stochastic trade-off. (e)–(g) Probability density distributions across experiments (number of realizations $N_r = 500$) of (e) branching times for different stochastic trade-off amplitudes (with dashed lines highlighting the shift in the peaks of the distributions), and fraction of acetate scavengers at different times for (f) $\sigma = 0$ and (g) $\sigma = 3 \times 10^{-4}$ (see Sec. IV of the SM [53]). The system's parameters for all the plots are $\beta = 0.25$ and those specified in the SM, Table I [53], where the shown $V_{g/a}$ are rescaled with respect to the table value as $V_{a/g} = \gamma V_{a/g}^{\text{table}}$ with $\gamma = 4.5 \times 10^{10}$. The stochastic trade-off parameters are $(a_{tr}, b_{tr}, c_{tr}, \tau) = (83.3, -3.5, 0.03, 10)$ (see Sec. V of the SM [53] for definitions and further information). Evolutionary simulations are carried out as described in Sec. III of the SM [53].

evolutionary picture is fully compatible with the one described in the experiments [15].

On the other hand, Fig. 2(d) summarizes the amount of realizations that starting from a glucose-specialist population and with the same parameters as in Fig. 2(a), ended up undergoing evolutionary branching at a maximum evolutionary time (arbitrarily fixed to $t_{\text{evo}}^{\max} = 3 \times 10^4$) for different amplitudes of the stochastic trade-off region, as obtained by varying the noise parameter σ for constant τ. In this way, by tuning the noise amplitude—or, equivalently, the flexibility of the metabolic constraints—the model is able to account for the experimental fact that diversification is observed in variable proportion of the experiments.

Furthermore, as shown in Figs. 2(e)–2(g), the model can also explain the empirically observed variability in both the branching times and the proportion of acetate scavengers after population splitting. Indeed, Fig. 2(e) reveals that branching times—estimated as explained in Sec. IV of the SM [53]—are variable and their distribution depends on the noise amplitude σ. One can observe that in the case with a "hard" trade-off (i.e., $\sigma = 0$), branching occurs almost always at the same time (strongly peaked distribution), but the standard deviation of the noise σ—or, equivalently, the amplitude of the trade-off—increases, where the distributions of branching times become wider and shift further to the right, corresponding to longer branching times. On the other hand, Fig. 2(f) shows that the distribution of the fraction of acetate scavengers at different times after branching is sharply peaked in the case with a hard trade-off, whereas the case of stochastic trade-off in Fig. 2(g) shows a much broader distribution.

As previously mentioned, the finite widths that emerge in the absence of stochasticity in the trade-off (i.e., for $\sigma = 0$)

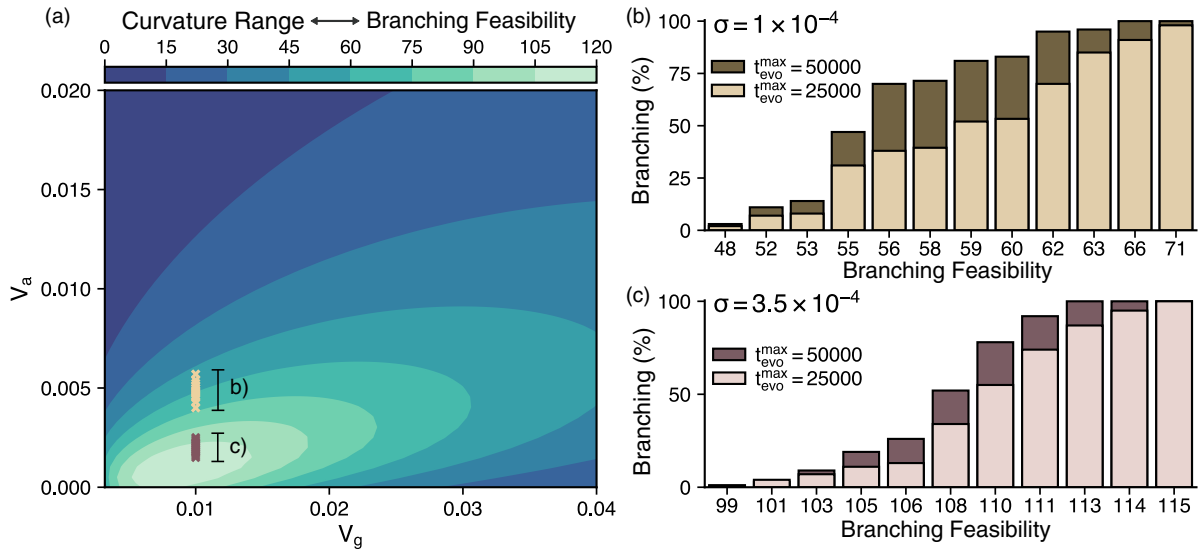

FIG. 3. Branching feasibility and the fraction of realizations that undergo branching. (a) Branching feasibility plot: contour plot that illustrates in phenotypic space the range of local curvatures of the hard trade-off that allows evolutionary branching. This curvature range can also be interpreted (with the stochastic trade-off idea) as the likeliness of having evolutionary branching at each point. (b),(c) Percentage of realizations (total number, $N_r = 200$) of the eco-evolutionary model with the stochastic trade-off that undergo evolutionary branching for two different maximum evolutionary times, $t_{evo}^{max} = 2.5\times10^4$ and $t_{evo}^{max} = 5\times10^4$, at different points in phenotypic space (that have different curvature range or, equivalently, different branching feasibility). Points in (b) are those in yellow in (a) and $\sigma = 10^{-4}$. Points in (c) are those in brown in (a) and $\sigma = 3.5\times10^{-4}$. The system's parameters are $\beta = 0.25$ and those specified in the SM, Table I [53], where the shown $V_{g/a}$ are rescaled with respect to the table value as $V_{a/g} = \gamma V_{a/g}^{table}$ with $\gamma = 4.5\times10^{10}$. The stochastic trade-off parameters are $\tau = 10$ and the others are obtained for each point shown in (a) as specified in Sec. II of the SM [53] with $\delta = 0.25$. Eco-evolutionary simulations are carried out as described in Sec. III of the SM [53].

arise from the limited time allowed for the ecological dynamics to stabilize. This is because we assume weak mutations, but not the infinitely weak mutation limit. As a result, clonal interference and the intrinsic randomness of the evolutionary algorithm may occur (see Sec. III of the SM [53]). We have computationally verified that the distributions gradually narrow as the time allowed for the ecological dynamics to reach equilibrium is extended (data not shown).

Therefore, assuming the data could be explained with a hard trade-off, one should see practically the same fraction for different realizations if measured at the same times, while assuming a stochastic trade-off, one should observe significant differences even if measured at same times. Although experimental data for branching times and fractions are scarce to allow for a quantitative comparison, our results suggest that the empirical observations are best represented by the stochastic case [16].

B. Branching feasibility and trade-off (in)dependence

As already discussed in Sec. I, the specific evolutionary outcomes of eco-evolutionary models crucially depend on the form of the trade-off [24,44]. Therefore, in order to generalize the results found in Sec. III A without relying on a specific form of the (mean) trade-off curve, one needs a framework that is able to discern whether a given ecological model equipped with a certain set of parameter values is able to undergo evolutionary branching (or not) independently of the specific form of the trade-off.

To this aim, we make use of the formalism proposed by de Mazancourt and Dieckmann [44]. As originally developed, such a framework allows one to analyze geometrically the possible evolutionary outcomes that can occur in the deterministic setting without imposing a specific mathematical function for the trade-off (for the sake of completeness, an overview of the method is described in Sec. I of the SM [53]). In particular, within this formalism, one can construct plots such as that of Fig. 3(a), providing information on how independent evolutionary branching is of the specific mathematical form of the hard trade-off. More specifically, it gives, at each point in phenotypic space, a measure of the range of possible local curvatures of the hard trade-off function that allows the model to undergo evolutionary branching at such a point, thus quantifying the robustness of branching against changes in the shape of the trade-off function (see Sec. I of the SM [53]). Regions where the range of possible local curvatures is small [deep blue in Fig. 3(a)] allow the model to undergo evolutionary branching deterministically only for very specific (fine-tuned) trade-off curves. Instead, in regions where the curvature range is high [light green in Fig. 3(a)], evolutionary branching occurs deterministically for a larger family of possible trade-off functions (see Sec. I of the SM [53] for further details).

Now, we would like to see how this (deterministic) formalism could be reinterpreted when we include the idea of stochastic trade-offs. It turns out that by using stochastic trade-offs, the previous plots [e.g., Fig. 3(a)] can be interpreted as *evolutionary-branching feasibility plots*, i.e., graphs showing the regions in phenotypic space where it is more likely to

see an evolutionary-branching event. In other words, regions in phenotypic space where branching is more robust against changes in the specific form of the hard trade-off correspond to regions in phenotypic space where branching is more likely to happen with the stochastic trade-off, and vice versa.

To justify this claim, we employ without loss of generality our eco-evolutionary model with a certain stochastic trade-off, whose average curve produces branching deterministically (i.e., in the $\sigma = 0$ limit) at a selected point in phenotypic space (see Sec. II of the SM [53] for further details of how the stochastic trade-off is built). Then, as illustrated in Figs. 3(b) and 3(c), points where deterministic branching depends weakly on the specific form of the hard trade-off—i.e., points where the range of local curvatures of the hard trade-off that allow branching is larger [brighter colors in Fig. 3(a)]—correspond, in the stochastic trade-off case, to more realizations that end up experiencing diversification at that point, and vice versa. Note, however, that in this framework, we can only work out the relative probabilities of branching. In other words, we can only indicate whether or not one branching condition is relatively more likely compared to another one.

Let us, however, remark that this mapping between the range of curvatures and feasibility of branching is quantitatively conditioned by the maximum evolutionary time of the realizations, $t_{\text{evo}}^{\text{max}}$. As both Figs. 3(b) and 3(c) show, the higher $t_{\text{evo}}^{\text{max}}$, the larger is the probability to observe evolutionary branching. This intuitive fact—i.e., the increase in the number of experiments that show diversification with the duration of such experiments—is indeed also observed experimentally [16]. Furthermore, Figs. 3(b) and 3(c) illustrate that the mapping is also quantitatively affected by the amplitude of the stochastic trade-off (controlled by σ). In agreement with Fig. 2(d), the smaller σ, the higher the probability of having evolutionary branching. In fact, in the hard trade-off limit where $\sigma = 0$ and the trade-off reduces to its average curve (which is chosen such that it undergoes branching), evolutionary branching occurs deterministically at almost the same times [as shown in Fig. 2(g)], independently of the point in phenotypic space.

Therefore, interpreting Fig. 3(a) as a branching-feasibility plot, we observe that branching is more likely for low values of V_a, which agrees with the reported picture of the evolution experiments given in [15]. As shown in Sec. III C of the SM [53], the specific contour pattern highly depends on the conditions of the experiment, that is, the concentration of glucose in the environment supplying the chemostat, G_0, the dilution rate d, and the proportion of the consumed glucose that gets excreted as acetate, β. Thus, Fig. 3(a) reveals essentially that the system, under these specific environmental conditions, is rather likely.

C. Theoretical predictions for different experimental values

As demonstrated, our model incorporating stochastic trade-offs effectively accounts for both the repeatability and variability of evolutionary branching observed in experimental data. Additionally, it provides insights into the regions in phenotypic space where branching is more likely to occur through the previously mentioned branching-feasibility plots. In this section, we illustrate how these plots can be interpreted to make theoretical predictions regarding the emergence of branching under different experimental conditions.

In particular, Figs. 4(a)–4(c) clearly illustrate that higher concentrations of glucose in the environment supplying the chemostat (G_0) generally increase the likelihood of branching. This is further verified in Fig. 4(d). Similar to Figs. 3(b) and 3(c), we use the same stochastic trade-off parameters for the three different environments whose average curve induces deterministic branching at a selected point. As evident in the histogram, the higher the glucose supply, the greater the number of realizations that undergo evolutionary branching. Moreover, the similarity in the contour pattern shape to that in Fig. 3(a) is attributed to the fact that the proportion of available acetate (i.e., β in this case) remains the same.

On the other hand, if an acetate concentration A_0 is added to the medium supplying the chemostat [Figs. 4(e)–4(g)], the pattern in the contour plot shifts and the likelihood of branching increases in different areas of the phenotypic space. This shift occurs because the added acetate concentration increases the proportion of available acetate (i.e., $\beta + A_0/G_0$). Figure 4(h) shows the number of realizations that undergo branching for the same stochastic trade-off in the three different environments, demonstrating that environments with higher acetate supply are more likely to experience branching.

Finally, it becomes clear from Figs. 4(i)–4(k) that the dilution rate is also a crucial parameter for the emergence of branching. Specifically, higher values of D significantly reduce the likelihood of branching, as illustrated in Fig. 4(l).

In summary, the proposed reinterpretation of the formalism developed by de Mazancourt and Dieckmann [44], incorporating stochastic trade-offs, not only generalizes our results to encompass a wider range of trade-offs, but also enables us to compare the likelihood of observing branching under different experimental conditions. This provides a deeper understanding of the theoretical foundations of branching and may help in making more accurate predictions as well, as in the design of future experiments.

IV. DISCUSSION

Understanding the mechanisms that generate, promote, and stabilize biological diversity stands as a challenging task. Microbiology experiments are particularly suited for this since the rapid adaptation/evolution of microorganisms allows one to empirically study evolution over relatively short time periods [57]. Here, we focused on a particular type of experimental setup in which a well-mixed isogenic population of *E. coli* is maintained on a glucose-limited chemostat over thousands of generations [14–16]. After a sufficient number of generations, a number of different experimental works report a splitting of the ancestor lineage into two different ecotypes (or strains) distinguished by their carbohydrate metabolism: the first one specializes in the consumption of glucose, while the second preferentially consumes a byproduct of glucose metabolism, i.e., acetate. This constitutes an illustrative example of the emergence of crossfeeding and the generation of complex communities/ecosystems even in the presence of few resources [49].

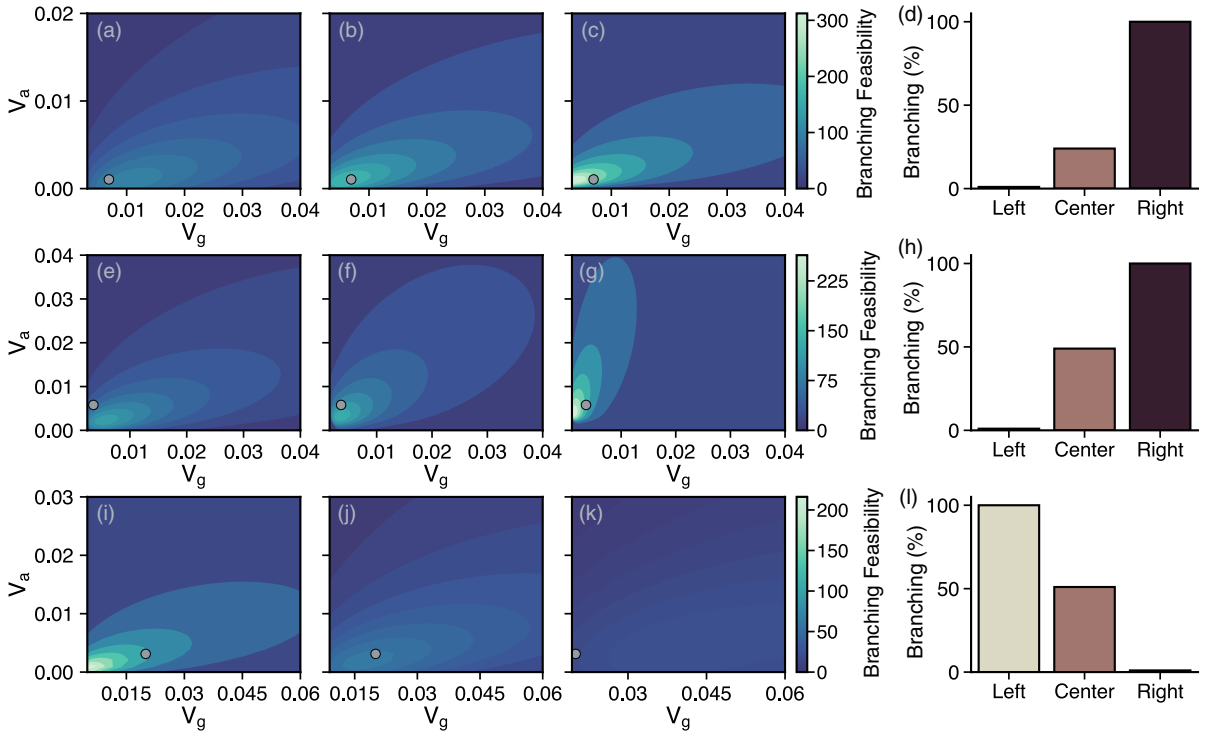

FIG. 4. Branching feasibility and the percentage of realizations that undergo branching for different experimental conditions. (a)–(c) Branching-feasibility plots for different values of glucose concentration in the environment supplying the chemostat: (a) $G_0 = 260$, (b) $G_0 = 694$, and (c) $G_0 = 3469$, all of them in μmol/L. (d) Number of realizations that undergo branching at the point depicted in (a)–(c) for the same stochastic trade-off with $(a_{tr}, b_{tr}, c_{tr}, \tau, \sigma) = (88.2, -2.5, 0.014, 10, 6\times10^{-4})$ (see the SM [53] for definitions and further information). (e)–(g) Branching-feasibility plots for different values of acetate concentration in the environment supplying the chemostat: (e) $A_0 = 100$, (f) $A_0 = 260$, and (g) $A_0 = 1000$, with all of them in μmol/L. (h) Number of realizations that undergo branching at the point depicted in (e)–(g) for the same stochastic trade-off with $(a_{tr}, b_{tr}, c_{tr}, \tau, \sigma) = (164.3, -3.6, 0.011, 10, 5\times10^{-4})$. (i)–(k) Branching-feasibility plots for different values of the dilution rate: (i) $D = 0.0015$, (j) $D = 0.006$, and (k) $D = 0.015$, with all of them in 1/min. (l) Number of realizations that undergo branching at the point depicted in (i)–(k) for the same stochastic trade-off with $(a_{tr}, b_{tr}, c_{tr}, \tau, \sigma) = (65.5, -5.6, 0.088, 10, 1.2\times10^{-4})$. The total number of realizations for the histograms is $N_r = 200$. The remaining parameters specified in the SM, Table I [53], where the shown $V_{g/a}$ are rescaled with respect to the table value as $V_{a/g} = \gamma V_{a/g}^{\text{table}}$ with $\gamma = 4.5\times10^{10}$.

Previous work [31] showed, in the context of adaptive dynamics, that a simple eco-evolutionary model can explain, in a parsimonious way, such a diversification event as the result of evolutionary branching. For this, one assumes a specific (hard) trade-off function between the evolving metabolic phenotypes, describing the relative preference for glucose, acetate, or a combination of both. Nevertheless, such an approach is deterministic in nature, i.e., either predicts that branching should be observed or not depending on the chosen trade-off analytical form. Therefore, it is not appropriate to explain the empirically observed stochasticity in the emergence of diversification and the variability both in branching times and in the relative weights of the emerging populations.

Alternatively, in this work, we propose the idea of a stochastic trade-off that stands as an effective representation of the underlying metabolic relations that constrain the evolution of bacteria in a high-dimensional phenotypic space. This high-dimensional space includes factors beyond those directly controlling metabolic preferences. The projection of a given mutational trajectory in such a high-dimensional manifold onto the two-dimensional phenotypic space of glucose-acetate preference does not need to be constrained to a simple curve (as illustrated in Fig. 1). Thus, instead of forcing the evolutionary trajectories in a lower-dimensional metabolic-preference space fixed trade-off curve, stochastic tradeoffs allow the populations to move in a wider region in such a space, introducing a new source of variability along such a space. In other words, the stochasticity of mutations in a high-dimensional feature space translates into variability that is not strictly constrained to a one-dimensional curve in the space of preferences, but rather to a flexible tradeoff curve. Mathematically, the stochastic trade-off is characterized by a central curve that stands as the average of the different trajectories, the correlation time τ that defines how fast the trajectories go back to this average curve and its amplitude, which, for fixed τ, is determined by σ and defines the width of the (fuzzy) region where populations can evolve.

Thus, we have built a biologically plausible eco-evolutionary model [see Eqs. (1)–(3)], fed with experimentally measured parameters (see the SM, Table I [53]) and equipped with the mentioned stochastic trade-off. We have shown that such a model is indeed able to account for the variability reported in the experiments (Fig. 2). In particular,

contrary to existing models, it does reproduce (i) the fact that branching occurs in a large proportion, but not all, of the realizations [Figs. 2(a)–2(d)], (ii) it may happen at considerably different times [Fig. 2(f)], and (iii) the fraction of acetate scavengers at a certain time is variable across experiments [Figs. 2(g) and 2(h)].

By reinterpreting the formalism of de Mazancourt and Dieckmann [44] with the concept of a stochastic trade-off, our model generalizes the results for a broader family of trade-offs. In addition, we have developed what we term the *branching-feasibility plot* [Fig. 3(a)], which quantifies the likelihood of branching at various points in phenotypic space for a general set of stochastic trade-offs. We have verified this by plotting the number of realizations that undergo evolutionary branching at different points in phenotypic space [Figs. 3(b) and 3(c)]. In summary, the branching-feasibility plot for our model indicates that for a wide range of stochastic trade-offs, this type of chemostat system is quite likely to undergo a diversification event, especially for low values of V_a. This justifies its repeated, albeit variable emergence in actual experiments.

It is also noteworthy that the framework we have devised here allows for theoretical predictions regarding the likelihood of observing branching under various experimental conditions. Indeed, in Fig. 4, we demonstrate how different experimental parameters can influence the probability of branching and how the region in phenotypic space where branching is most likely can vary. Specifically, we have shown that increasing the amount of glucose and/or acetate supplied to the system makes evolutionary branching more likely, whereas increasing the dilution rate can make branching almost impossible. Therefore, this framework provides us with a deeper theoretical understanding of the factors controlling diversification in real experiments. Furthermore, predictions from the model can be easily tested experimentally by repeating the evolutionary experiments under different conditions and comparing the percentage of realizations that result in diversification.

The theoretical analyses made in this work assume, as is customary in adaptive dynamics, that evolutionary changes are perturbative in phenotypic space, i.e., phenotypes change gradually. However, this might not be the case for actual evolutionary experiments with bacteria. For example, one can imagine that mutations in certain genes could confer on an initially glucose-limited bacterial population the ability to metabolize finite amounts of acetate without having to wait for many generations. Future work will therefore be devoted to implementing this possibility in the models and exploring how it can possibly change the overall picture. Finally, as mentioned in Sec. I, the repeated branching of an ancestor *E. coli* lineage into two distinct ecotypes characterized by their carbohydrate metabolism is also observed in serial dilution experiments in which bacteria evolve in a batch of glucose-acetate [10,11,17,35–38]. The framework introduced here can be easily adapted to such a scenario and further work will be devoted to it. We believe that the ideas introduced here—in particular the idea of stochastic trade-offs—will motivate further research into understanding the underlying principles of evolution under controlled conditions.

ACKNOWLEDGMENTS

This work has been supported by Grant No. PID2020-113681GB-I00 of the Spanish Ministry and Agencia Estatal de Investigación MICIU/AEI/10.13039/501100011033. It has also been supported by Grant No. PID2023-149174NB-I00 financed by MICIU/AEI/10.13039/501100011033 and ERDF funds. R.C.L. acknowledges funding from the Spanish Ministry and AEI, under Grant No. FPU19/03887 and from the Arqus Alliance of European Universities program 6.5. S.A. acknowledges the support of the NBFC to the University of Padova, funded by the Italian Ministry of University and Research, PNRR, Missione 4 Componente 2, "Dalla ricerca all'impresa," Investimento 1.4, Project No. CN00000033. S.S. acknowledges financial support under the National Recovery and Resilience Plan (NRRP), Mission 4, Component 2, Investment 1.1, Call for Tender No. 104 by the Italian Ministry of University and Research (MUR), funded by the European Union—NextGenerationEU—Project Title: Anchialos: Diversity, function, and resilience of Italian coastal aquifers upon global climatic changes—CUP C53D23003420001 Grant Assignment Decree No. 1015 adopted by the Italian Ministry of Ministry of University and Research (MUR). The authors warmly thank Amos Maritan for insightful discussions and for contributions to the early stages of this research.

[1] C. Darwin, *On the Origin of Species, 1859* (John Murray, London, 2004).

[2] G. E. Hutchinson, Homage to Santa Rosalia or why are there so many kinds of animals? Am. Natur. **93**, 145 (1959).

[3] S. J. Gould, *The Structure of Evolutionary Theory* (Harvard University Press, Harvard, MA, 2002).

[4] H. J. Muller, Isolating mechanisms, evolution, and temperature, in *Biological Symposia Volume 6: Temperature and Evolution: Isolating Mechanisms: Genetic Control of Embryonic Development*, edited by T. Dobzhansky (Jacques Cattell Press, Lancaster, Pennsylvania, 1942), pp. 71–125.

[5] E. Mayr, *Animal Species and Evolution* (Belknap Press of Harvard University Press, Harvard, MA, 1963).

[6] T. Dobzhansky, *Genetics of the Evolutionary Process* (Columbia University Press, Columbia, NY, 1970).

[7] J. Coyne, Genetics and speciation, Nature (London) **355**, 511 (1992).

[8] M. Turelli, N. H. Barton, and J. A. Coyne, Theory and speciation, Trends Ecol. Evolut. **16**, 330 (2001).

[9] P. B. Rainey and M. Travisano, Adaptive radiation in a heterogeneous environment, Nature (London) **394**, 69 (1998).

[10] M. Friesen, G. Saxer, M. Travisano, and M. Doebeli, Experimental evidence for sympatric ecological diversification due to frequency-dependent competition in escherichia coli, Evolution **58**, 245 (2003).

[11] J. Tyerman, N. Havard, G. Saxer, M. Travisano, and M. Doebeli, Unparallel diversification in bacterial microcosms, Proc. Biol. Sci. USA **272**, 1393 (2005).

[12] R. Craig Maclean, Adaptive radiation in microbial microcosms, J. Evolut. Biol. **18**, 1376 (2005).

[13] G. Saxer, M. Doebeli, and M. Travisano, The repeatability of adaptive radiation during long-term experimental evolution of *escherichia coli* in a multiple nutrient environment, PLoS ONE **5**, e14184 (2010).

[14] R. Helling, C. Vargas, and J. Adams, Evolution of escherichia coli during growth in a constant environment, Genetics **116**, 349 (1987).

[15] R. Rosenzweig, R. Sharp, D. Treves, and J. Adams, Microbial evolution in a simple unstructured environment: Genetic differentiation in *escherichia coli*, Genetics **137**, 903 (1994).

[16] D. Treves, S. Manning, and J. Adams, Repeated evolution of an acetate-crossfeeding polymorphism in long-term populations of *escherichia coli*, Mol. Biol. Evol. **15**, 789 (1998).

[17] D. Rozen and R. Lenski, Long-term experimental evolution in *escherichia coli*. VIII. Dynamics of a balanced polymorphism, Am. Nat. **155**, 24 (2000).

[18] C. Linn, J. Feder, S. Nojima, H. Dambroski, S. Berlocher, and W. Roelofs, Fruit odor discrimination and sympatric host race formation in Rhagoletis, Proc. Natl. Acad. Sci. USA **100**, 11490 (2003).

[19] M. Barluenga, K. Stölting, W. Salzburger, M. Muschick, and A. Meyer, Sympatric speciation in Nicaraguan crater lake cichlid fish, Nature (London) **439**, 719 (2006).

[20] V. Savolainen, M. C. Anstett, C. Lexer, I. Hutton, J. J. Clarkson, M. V. Norup, M. P. Powell, D. Springate, N. Salamin, and W. J. Baker, Sympatric speciation in palms on an oceanic island, Nature (London) **441**, 210 (2006).

[21] P. G. Ryan, P. Bloomer, C. L. Moloney, T. J. Grant, and W. Delport, Ecological speciation in South Atlantic island finches, Science **315**, 1420 (2007).

[22] B. Bayramoglu, D. Toubiana, S. Van Vliet, R. F. Inglis, N. Shnerb, and O. Gillor, Bet-hedging in bacteriocin producing *escherichia coli* populations: The single cell perspective, Sci. Rep. **7**, 42068 (2017).

[23] S. A. H. Geritz, J. A. J. Metz, E. Kisdi, and G. Meszéna, Dynamics of adaptation and evolutionary branching, Phys. Rev. Lett. **78**, 2024 (1997).

[24] S. Geritz, E. Kisdi, G. Meszena, and J. Metz, Evolutionarily singular strategies and the adaptive growth and branching of the evolutionary tree, Evol. Ecol. **12**, 35 (1998).

[25] J. A. J. Metz, S. A. H. Geritz, G. Meszena, F. J. A. Jacobs, and J. S. van Heerwaarden, Adaptive dynamics: A geometrical study of the consequences of nearly faithful replication, in *Stochastic and Spatial Structures of Dynamical Systems*, edited by S. J. van Strien and S. M. Verduyn Lunel (North Holland, Amsterdam, 1996), pp. 183–231.

[26] U. Dieckmann and R. Law, The dynamical theory of coevolution: A derivation from stochastic ecological processes, J. Math. Biology **34**, 579 (1996).

[27] M. Doebeli, *Adaptive Diversification* (Princeton University Press, Princeton, NJ, 2011).

[28] U. Dieckmann and M. Doebeli, On the origin of species by sympatric speciation, Nature (London) **400**, 354 (1999).

[29] A. G. Stefan, É. Kisdi, and P. Yan, Evolutionary branching and long-term coexistence of cycling predators: Critical function analysis, Theor. Popul. Biol. **71**, 424 (2007).

[30] H. Ito and A. Sasaki, Evolutionary branching under multi-dimensional evolutionary constraints, J. Theor. Biol. **407**, 409 (2016).

[31] M. Doebeli, A model for the evolutionary dynamics of cross-feeding polymorphisms in microorganisms, Popul. Ecol. **44**, 59 (2002).

[32] É. Kisdi and S. A. H. Geritz, Adaptive dynamics: A framework to model evolution in the ecological theatre, J. Math. Biol. **61**, 165 (2010).

[33] U. Dieckmann, M. Doebeli, J. Metz, and D. Tautz, *Adaptive Speciation*, Cambridge Studies in Adaptive Dynamics (Cambridge University Press, Cambridge, UK, 2004).

[34] M. Sireci and M. A. Muñoz, Statistical mechanics of phenotypic eco-evolution: From adaptive dynamics to complex diversification, Phys. Rev. Res. **6**, 023070 (2024).

[35] C. Spencer, M. Bertrand, M. Travisano, and M. Doebeli, Adaptive diversification in genes that regulate resource use in *escherichia coli*, PLoS Genet. **3**, e15 (2007).

[36] C. C. Spencer, J. Tyerman, M. Bertrand, and M. Doebeli, Adaptation increases the likelihood of diversification in an experimental bacterial lineage, Proc. Natl. Acad. Sci. USA **105**, 1585 (2008).

[37] M. Le Gac, M. Brazas, M. Bertrand, J. Tyerman, C. Spencer, R. Hancock, and M. Doebeli, Metabolic changes associated with adaptive diversification in *escherichia coli*, Genetics **178**, 1049 (2008).

[38] M. Herron and M. Doebeli, Parallel evolutionary dynamics of adaptive diversification in escherichia coli, PLoS Biol **11**, e1001490 (2013).

[39] M. Tikhonov, S. Kachru, and D. S. Fisher, A model for the interplay between plastic tradeoffs and evolution in changing environments, Proc. Natl. Acad. Sci. USA **117**, 8934 (2020).

[40] R. Schuetz, N. Zamboni, M. Zampieri, M. Heinemann, and U. Sauer, Multidimensional optimality of microbial metabolism, Science **336**, 601 (2012).

[41] O. Shoval, H. Sheftel, G. Shinar, Y. Hart, O. Ramote, A. Mayo, E. Dekel, K. Kavanagh, and U. Alon, Evolutionary trade-offs, Pareto optimality, and the geometry of phenotype space, Science **336**, 1157 (2012).

[42] S. C. Stearns, Trade-offs in life-history evolution, Funct. Ecol. **3**, 259 (1989).

[43] T. Garland, Trade-offs, Curr. Biol. **24**, R60 (2014).

[44] C. de Mazancourt and U. Dieckmann, Trade-off geometries and frequency-dependent selection, Am. Nat. **164**, 765 (2004).

[45] M. Amicone and I. Gordo, Molecular signatures of resource competition: Clonal interference favors ecological diversification and can lead to incipient speciation, Evolution **75**, 2641 (2021).

[46] B. H. Good, S. Martis, and O. Hallatschek, Adaptation limits ecological diversification and promotes ecological tinkering during the competition for substitutable resources, Proc. Natl. Acad. Sci. USA **115**, E10407 (2018).

[47] M. M. Desai and D. S. Fisher, Beneficial mutation–selection balance and the effect of linkage on positive selection, Genetics **176**, 1759 (2007).

[48] I. Gudelj, M. Kinnersley, P. Rashkov, K. Schmidt, and F. Rosenzweig, Stability of cross-feeding polymorphisms in microbial communities, PLoS Comput. Biol. **12**, e1005269 (2016).

[49] C. Liao, T. Wang, S. Maslov, and J. B. Xavier, Modeling microbial cross-feeding at intermediate scale portrays community dynamics and species coexistence, PLoS Comput. Biol. **16**, e1008135 (2020).

[50] M. Basan, S. Hui, H. Okano, Z. Zhang, Y. Shen, J. Williamson, and T. Hwa, Overflow metabolism in *escherichia coli* results from efficient proteome allocation, Nature (London) **528**, 99 (2015).

[51] J. Monod, The growth of bacterial cultures, Annu. Rev. Microbiol. **3**, 371 (1949).

[52] Analytical solutions to this problem are often challenging, so one frequently resorts to pairwise invasibility plots for insights (see [24,58] for further details).

[53] See Supplemental Material at http://link.aps.org/supplemental/10.1103/PhysRevResearch.6.043199 for further details about the methodology and computational results, which includes Refs. [58–63].

[54] J. Y. Wakano and Y. Iwasa, Evolutionary branching in a finite population: Deterministic branching vs. stochastic branching, Genetics **193**, 229 (2013).

[55] R. Caetano, Y. Ispolatov, and M. Doebeli, Evolution of diversity in metabolic strategies, eLife **10**, e67764 (2021).

[56] D. A. Roff and D. J. Fairbairn, The evolution of trade-offs: Where are we? J. Evolut. Biol. **20**, 433 (2007).

[57] B. Van den Bergh, T. Swings, M. Fauvart, and J. Michiels, Experimental design, population dynamics, and diversity in microbial experimental evolution, Microbiol. Molec. Biol. Rev. **82**, e00008-18 (2018).

[58] Å. Brannstrom, J. Johansson, and N. Von Festenberg, The hitchhiker's guide to adaptive dynamics, Games **4**, 304 (2013).

[59] J. E. Goldford, N. Lu, D. Bajií, S. Estrela, M. Tikhonov, A. Sanchez-Gorostiaga, D. Segrè, P. Mehta, and A. Sanchez, Emergent simplicity in microbial community assembly, Science **361**, 469 (2018).

[60] C. Rueffler, T. Van Dooren, and J. Metz, Adaptive walks on changing landscapes: Levins approach extended, Theor. Popul. Biol. **65**, 165 (2004).

[61] R. G. Bowers, A. Hoyle, A. White, and M. Boots, The geometric theory of adaptive evolution: Trade-off and invasion plots, J. Theor. Biol. **233**, 363 (2005).

[62] E. Kisdi, Trade-off geometries and the adaptive dynamics of two co-evolving species, Evolut. Ecol. Res. **8**, 959 (2006).

[63] R. Lande, Natural selection and random genetic drift in phenotypic evolution, Evolution **30**, 314 (1976).